Design and Test of an Axial Flux Permanent-Magnet Machine With Field Control Capability

Delvis A. González-Lopez[1], Juan A. Tapia[2], Rogel Wallace[2], and Anibal Valenzuela[2]

[1]Direct Drive Systems, Cerritos, CA 90703 USA
[2]Department of Electrical Engineering, University of Concepcion, Concepcion, Chile

We designed and tested a new axial flux permanent-magnet machine (AFPM) with field weakening capability. This paper provides a summary of key design features, optimization, and test results of an AFPM prototype. The proposed field weakening method is based on the control of the d-axis component of the armature reaction flux. The paper focuses on the air-gap flux control capability of the topology.

***Index Terms*—Axial flux machine, field weakening, permanent-magnet machines.**

I. Introduction

AXIAL FLUX permanent-magnet (AFPM) machines have gained popularity in the last few decades because of their higher torque at low speed and better power density compared with radial flux machines [1], [2]. The main applications where these features are attractive are traction [3] and energy generation. AFPM topologies offer the possibility to design a high pole machine. Therefore, it can be directly coupled to the turbines in low-speed energy systems, such as wind and hydro generators [4], [5].

Additionally, the absence of excitation windings and brush contact reduce the operational cost and increase the efficiency and reliability. However, the fixed flux imposed by the magnets becomes crucial for variable speed applications. The linear variation of the induced voltage [back-electromotive force (EMF)] with the frequency makes their operation dangerous at high speed. In fact, the winding insulation and inverter power semiconductor can be degraded when operated at high voltage. In order to avoid this unsafe operation, air-gap flux control must be performed to keep the terminal voltage at rated value.

To overcome this problem, several topologies of surface-mounted permanent-magnet (PM) machines had been proposed in the literature [6], [7]. In those cases, extra windings are considered to generate an additional dc flux component. As a result, the total excitation flux is a combination between the magnet and dc flux components.

A powerful tool to command air-gap flux is vector control. With this technique, it is possible to inject a negative d-axis flux commanding the stator vector current to control the total air-gap flux. However, due to the high d-axis reluctance in surface-mounted permanent-magnet machines, an elevated current is required to perform adequate flux control. As a result, an intense demagnetization flux is exercised against the magnet and the generated heat by the current increase in the machine temperature. Both effects should cause an irreversible degradation of magnet properties. Nevertheless, a design consideration can be present to reach the field weakening operation with low d-axis Ampere-turns, reducing the rotor demagnetization risk.

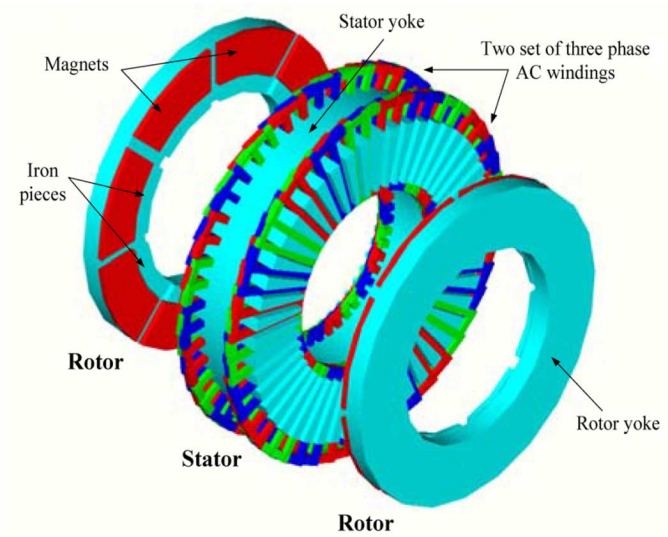

Fig. 1. Proposed AFPM machine topology.

In this paper, a novel 5 kVA 8-pole AFPM prototype presented in [8] is experimentally evaluated. The tests were carried out in the Electrical Machines Laboratory of University of Concepcion and were focused to validate the flux control theory proposed and the field weakening capability of the prototype.

II. Presented Topology

The axial flux surface-mounted PM machine topology assembled is depicted in Fig. 1. This is a double rotor and central stator configuration with North–North magnetization.

The stator contains two sets of three-phase ac windings. Each winding can be controlled independently so that the machine becomes two magnetic structures (motors) connected by the shaft. The rotor pole is a combination of a rare earth magnet (neodymium–iron–bore) and soft laminated iron so the total d-axis reluctance is reduced. Both stator and rotor yokes were laminated as spiral to minimize radial flux component circulation. The lamination of the iron piece reduces the leakage flux on the rotor pole. Flux distribution on the machine is greatly defined by the stator teeth geometry (trapezoidal to keep slot rectangular). In fact, as the tooth width diminishes (closer to the shaft), the iron tooth becomes continuously more saturated due to magnet presence. To improve laminated iron utilization, the

Digital Object Identifier 10.1109/TMAG.2008.2000543

Color versions of one or more of the figures in this paper are available online at http://ieeexplore.ieee.org.

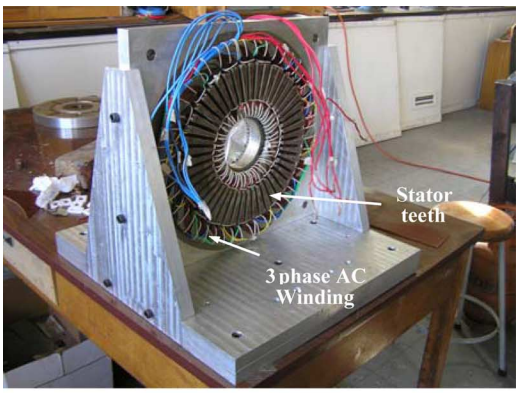

a)

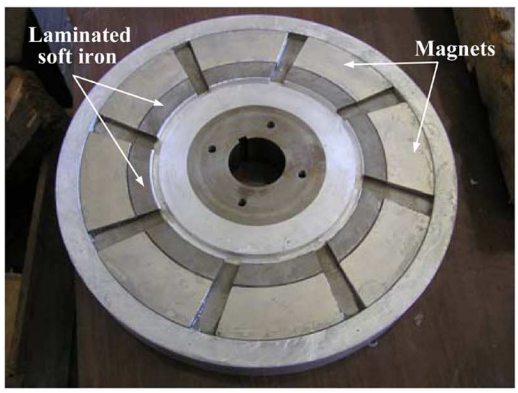

b)

Fig. 2. A 5 kVA, 8-pole axial flux PM prototype. (a) Stator core with three-phase windings. (b) Rotor with PM and iron pieces.

TABLE I
PROTOTYPE DIMENSIONS

Quantity	Value
Outer diameter	282 mm
PM diameter	180 mm
Inner diameter	170 mm
Stack length	115 mm
Slots	48
Teeth width	7 mm
Slot depth	20 mm

rotor yoke is manufactured following a trapezoidal geometry. In this manner, a better flux density profile is found and the total flux in the machine is increased. Following these design features, a prototype was built. Table I lists the main dimensions and Fig. 2(a) and (b) depicts the stator and rotor, respectively.

III. FLUX CONTROL CONCEPT

A. Operating Principle

The rotor pole design allows an easy air-gap flux control using the *d*-axis armature current control. The soft iron piece over the rotor surface offers a low reluctance path for the armature reaction flux and magnets are not subjected to a demagnetization field.

Fig. 3 depicts the phasors diagram for operation over a rated speed. The air-gap flux reduction can be obtained with proper control of the current vector angle (γ). The resultant air-gap flux in *d*-axis will be the difference between excitation and the injecting armature reaction flux. The induced voltage (E_f) and the voltage drop $(\mathrm{j}X_dI_d)$ increase with the speed. Because the opposite direction of the vectors E_f and $\mathrm{j}X_dI_d$ the terminal voltage (V_t) still in rated value for extended speed operation.

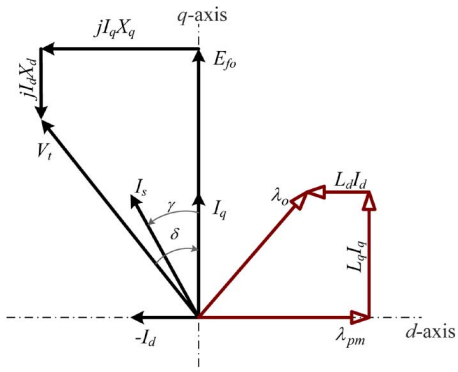

Fig. 3. Phasor diagram and flux relationship for extended speed operation.

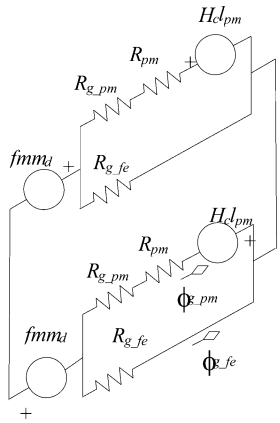

Fig. 4. Magnetic equivalent circuit for the AFPM topology proposed.

Considering one pole magnetic equivalent circuit, depicted in Fig. 4, it is possible to evaluate the air-gap flux in term of the machine parameters.

For this analysis it was assumed that the air-gap flux has two components: the flux in front of the magnet, ϕ_{g_pm}, and the flux in front of the iron pole, ϕ_{g_fe}. Magnet leakage and iron reluctance are neglected. Since magnet permeability is close to unity, then $R_{g\_\mathrm{pm}} + R_{\mathrm{pm}} \gg R_{g\_\mathrm{fe}}$ therefore, each component of the air-gap flux can be expressed as

$$\phi_{g\_\mathrm{pm}} \cong \frac{H_c l_{\mathrm{pm}}}{R_{g\_\mathrm{pm}} + R_{\mathrm{pm}}} \tag{1}$$

$$\phi_{g\_\mathrm{fe}} \cong \frac{fmm_d}{R_{g\_\mathrm{fe}}}. \tag{2}$$

In (2), fmm_d is the equivalent *d*-axis armature reaction magnetomotive force (MMF) provided by the stator current. The total air-gap flux is the combination of these two components

$$\phi_g = \phi_{g\_\mathrm{fe}} + \phi_{g\_\mathrm{pm}}. \tag{3}$$

And the reluctances are defined by

$$R_{g\_\mathrm{pm}} = \frac{2g}{\mu_o A_{\mathrm{pm}}} \tag{4}$$

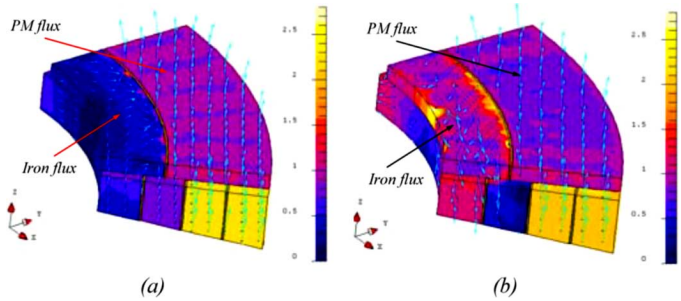

Fig. 5. Air-gap flux distribution for (a) no-load condition, (b) on load with rated stator current oriented to d-axis (maximum demagnetization).

$$R_{g\_\mathrm{fe}} = \frac{2g}{\mu_o A_{\mathrm{fe}}} \tag{5}$$

$$R_{\mathrm{pm}} = \frac{2l_{\mathrm{pm}}}{\mu_{\mathrm{pm}}\mu_o A_{\mathrm{pm}}} \tag{6}$$

where

g	air-gap length;
A_{pm}	magnet area facing the air gap;
A_{fe}	soft iron pole area facing the air gap;
l_{pm}	magnet axial length;
H_c	magnet coercive magnetic force;
μ_{pm}	magnet permeability.

From (1) and (2), it can be noticed that each component is magnetized by a different flux source. The magnet section is excited by PM ($H_c l_{\mathrm{pm}}$) and the magnetic circuit is composed by air gap, stator, and rotor cores and magnet. On the other hand, the d-axis armature reaction component (fmm_d) excites the iron section of the rotor pole. The magnitude and direction of this flux is commanded by the proper stator current vector. The magnetic circuit for this flux is air-gap, stator and rotor cores, and iron section of the rotor pole. Neglecting saturation, both magnetic circuits are independent, resulting in no effect of armature reaction over the magnet (no demagnetization risk) and a low current requirement to impose flux in the soft iron rotor pole section. As a result, total air-gap flux can be adjusted controlling a d-axis armature reaction flux, increasing or decreasing its magnitude according to the speed operation.

B. Finite-Element (FE) Analysis

In order to verify the air-gap flux control capability of the proposed topology, a FE analysis was carried out using professional software FLUX 3D. In Fig. 5, air-gap flux distribution is depicted for no-load and for rated armature current at d-axis (maximum demagnetizing effect). For no stator current condition, the air-gap flux is only due to the magnet [Fig. 5(a)]. The iron section is almost free of magnetization and only the flux is present due to the magnet leakage. The stator and rotor yokes lamination helps reduce this component. Therefore, a solid yoke is not recommended for this application. When stator current is present, an additional d-axis flux component flows in the same magnet axis. As Fig. 5(b) depicts, most of the armature reaction flux circulates through the iron section with minor effect over the magnets.

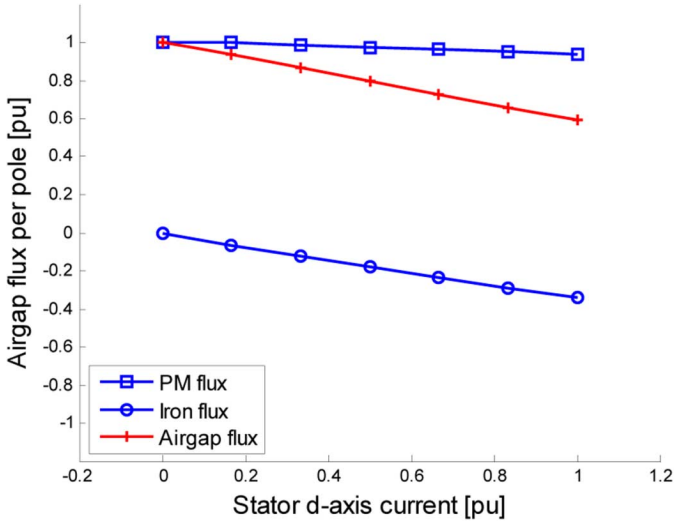

Fig. 6. Air-gap flux distribution for demagnetizing effect versus d-axis current. (Iron/PM areas ratio 0.35).

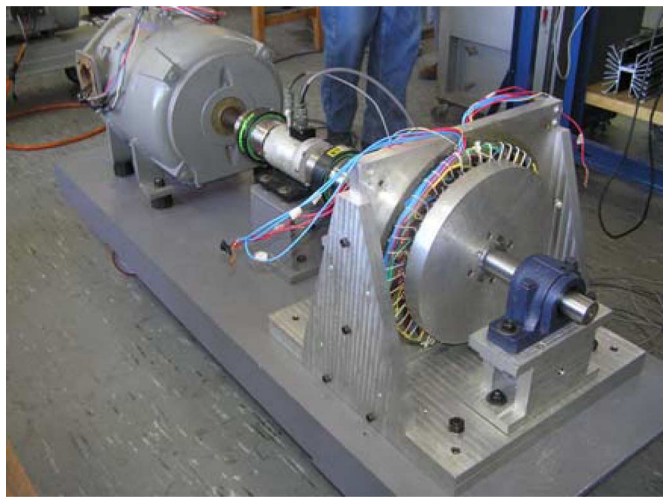

Fig. 7. Test lab setup for the 5 kVA, 8-pole AFPM prototype.

In order to estimate the evolution of the air-gap flux as a function of d-axis current, iron and magnet flux are calculated independently. In Fig. 6, each component is plotted for an iron to magnet areas ratio equal 0.35. This result shows that magnet flux density is almost constant as the stator current increases (d-axis). Consequently, flux density over iron section pole varies linearly respect to stator current. For the particular design analyzed the maximal demagnetization expected is about 40%.

IV. Performed Tests and Results

To validate the operational properties of the machine concept presented, a 5 kVA, 8-pole AFPM prototype with the proposed rotor configuration was built and tested. Fig. 7 depicts the laboratory test setup. A dc machine was used as a load or prime motor to get the desired prototype operation mode (generator or motor). Proper torque, current, and voltage sensors are utilized to measure the significant mechanic and electrical parameters.

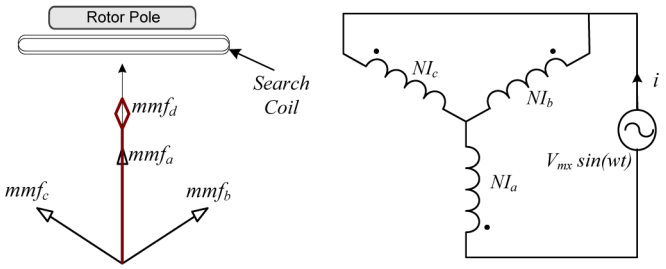

Fig. 8. Rotor locked test to determine air-gap flux under demagnetizing effect of armature reaction.

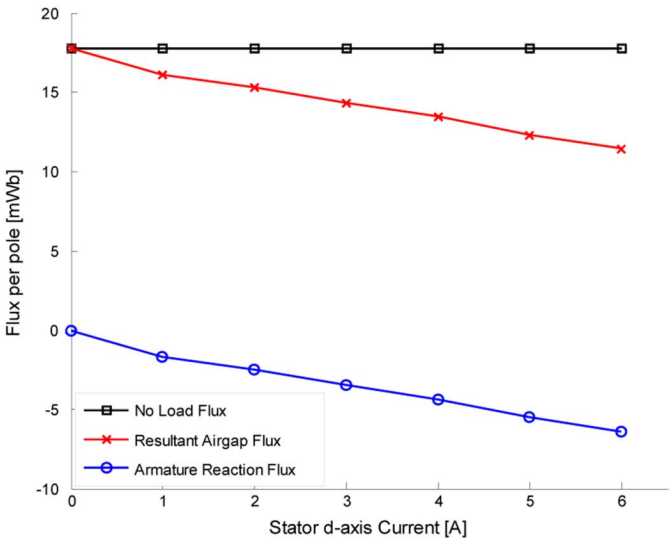

Fig. 9. Flux weakening capability injecting *d*-axis current.

A. Locked Rotor Test

In order to verify the field control capability, a span search coil was placed in the stator teeth to measure one pole air-gap flux. With *d*-axis aligned with the search coil, the rotor was locked and 50 Hz single-phase voltage was applied to the three-phase stator windings, connected according to the circuit in Fig. 8. A stator MMF was applied directly to *d*-axis rotor pole (magnet and soft iron pieces). The induced voltage in the search coil was measured for several current magnitudes. By numerical integration, the air-gap flux per pole was calculated in each case. Since the rotor is locked, there is no induced voltage associated to the magnet flux in the search coil.

From no-load generator test, a 50 Hz induced voltage in the search coil was measured. Since there is no armature reaction flux, the obtained voltage is only produced by the magnet excitation flux. The air-gap flux was calculated from the voltage waveform. A first approximation to the air-gap flux reduction is the combination of these two components. In this approach, magnet MMF drop was neglected.

The resultant air-gap flux components are depicted in Fig. 9. Finally, the total air-gap flux can be reduced up to a 62.0%. Due to the soft iron piece in the rotor pole, *d*-axis armature reaction flux can penetrate easily in the rotor, achieving important control range for the machine excitation.

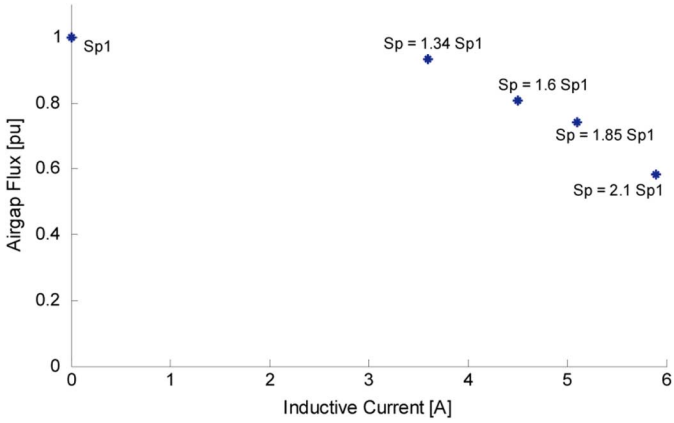

Fig. 10. Flux weakening capability as a generator, with inductive load.

B. Generator Test With Inductor Load Bank

Using the laboratory setup presented in Fig. 7, a loaded generator test was carried out. The three-phase load was composed by a variable inductor bank connected in parallel with a variable resistor bank. The inductive current causes a displacement of the stator current vector toward negative *d*-axis (demagnetizing effect).

The test consisted of increasing the speed while the terminal voltage and current values remain in 1.0 pu. With only a resistor load bank connected, the speed, rated current, and voltage were archived. Then, the speed was increased while the inductance/resistance ratio of the load was adjusted. In every step, the total air-gap flux per pole was measured with the search coil.

Fig. 10 depicts the archived air-gap flux versus the inductive current. The air-gap flux was reduced to 58.0% when only the inductive load was connected. The speed (S_p) was increase 2.1 times while the terminal voltage remains in 1.0 pu.

C. Inductance Profiles

Using a locked rotor test, *dq*-axis inductances can be estimated based on voltage and current measurements. The rotor was aligned with stator *d*-axis and *q*-axis, respectively. Fig. 11 illustrates the inductance variation as a function of its corresponding currents. The test results are compared with the inductance values obtained by 3D-FE analysis.

At first sight, it can be noticed that the magnetic saliency exhibited by the machine corresponds to a regular wound salient pole rotor synchronous machine, where $L_d > L_q$. Due to magnet permeability, the regular surface mounted PM machines exhibits no saliency. The magnets are located at *d*-axis flux path; as a result, their reluctance becomes predominant respect to the air-gap reluctance. However, for the current case, presence of an iron pole section at the rotor pole exchanges the regular saliency expected in a PM machine. The parallel combination of both materials makes predominant the soft iron permeability, resulting in a low armature Ampere-turn requirement to reduce air-gap flux.

At the same time, iron saturation plays an important role in defining operational *d*-axis inductance. In fact, magnet residual

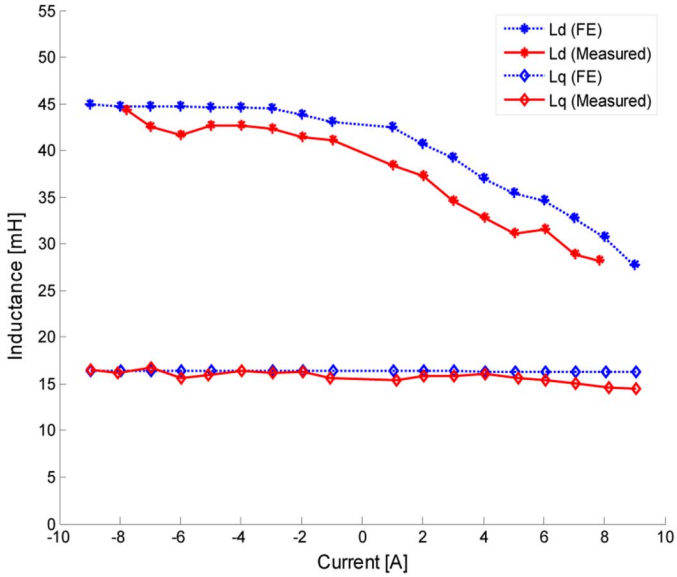

Fig. 11. *dq-axes* inductances variation with respect to the stator current. Magnetizing and demagnetizing effect of the armature reaction.

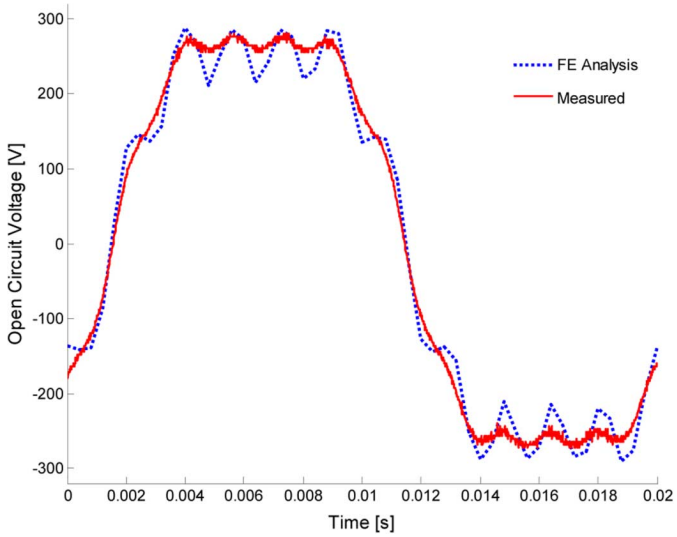

Fig. 12. Measurement and 3D-FE resultant open circuit voltage.

flux density saturates the magnetic circuit, establishing an asymmetrical flux linkage distribution for magnetizing and demagnetizing current action. This effect is observed in Fig. 11 as well, where the inductance has a clear dependency on the magnitude and direction of the stator current. In contrast, q -axis inductance shows only a minor variation. The large *interpolar* air gap and no magnet along this path make the direction of the stator MMF indifferent. The saliency ratio, defined as the quotient between L_d and L_q, varies between 2 to 3 depending on load conditions.

D. Induced Voltage

Close agreement was found between measured and predicted no load induced phase voltage waveforms, as depicted in Fig. 12. Both curves have a trapezoidal waveform due to the magnet excitation.

The variation of the stator reluctance by the slots brings out a pulsating component in the back-EMF waveform. Then, a harmonic analysis is carried out and is shown in Fig. 13. The third harmonic is about 17.0% of the fundamental component, caused by the trapezoidal waveform of the induced voltage. But it disappears in a Y-connection winding without neutral wire. Other significant harmonics, like eleven and thirteen, are produced by the pulsating component in the simulated waveform. Nevertheless, the pulsation amplitude in the measured waveform is low, and thus, the introduced high-order harmonics are reduced.

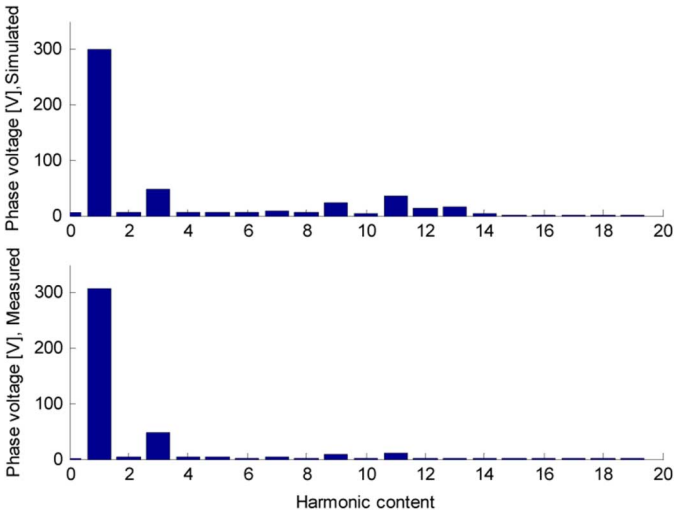

Fig. 13. Harmonic content of simulated and measured phase induced voltage.

V. Conclusion

In this paper, an experimental validation of a novel 5 kVA, 8-pole axial flux PM machine with field weakening capability is presented. Main magnetic circuit modifications allow reducing the magnitude of stator Ampere-turn required to control the air-gap flux. In fact, the soft iron section of the rotor pole reduces reluctance, resulting in a low d-axis stator current requirement to demagnetize the machine with low magnetic and thermal stress for the magnet. Additionally, a procedure to evaluate this feature was implemented. With this approach, over 40% air-gap reduction can be achieved using an armature reaction as a control mechanism.

A close agreement was found between 3D-FE analysis and test results for inductances and induced voltage. Inverse saliency profile was presented in an AFPM prototype in contrast with a regular PM machine. Because of the two section rotor pole, the d-axis inductance is larger than the q-axis one. The saturation effect causes a saliency variation according to load conditions.

Acknowledgment

The authors wish to acknowledge the financial support provided by the Direccion de Investigacion of the Universidad de Concepcion, through Proyecto DIUC No 206.092.047-1.0, and the Chilean Fund for Scientific and Technological Development (FONDECYT), through project No. 1070493.

References

[1] A. Parviainen, M. Niemelä, J. Pyrhönen, and L. J. Mantere, "Performance comparison between low-speed axial-flux and radial-flux permanent magnet machines including mechanical constraints," in *IEEE Int. Electric Machines and Drives Conf., IEMDC*, May 2005.

[2] R. Qu, M. Aydin, and T. A. Lipo, "Performance comparison of dual-rotor radial-flux and axial-flux permanent-magnet BLDC machines," in *IEEE Int. Electric Machines and Drives Conf., IEMDC.*, May 2003.
[3] Y.-P. Yang and D. S. Chuang, "Optimal design and control of a wheel motor for electric passeneger cars," *IEEE Trans. Magn.*, vol. 43, no. 1, pp. 51–61, Jan. 2007.
[4] S. M. Hosseini, M. Agha-Mirsalim, and M. Mirzaei, "Design, prototyping, and analysis of low cost axial-flux coreless permanent-magnet generator," *IEEE Trans. Magn.*, vol. 44, no. 1, pp. 75–80, Jan. 2008.
[5] Y. Chen, P. Pillay, and A. Khan, "PM wind generator comparison of different topologies," in *IEEE Ind. Appl. Annual Meeting*, Oct. 2004.
[6] J. A. Tapia, F. Leonardi, and T. A. Lipo, "Consequent-pole permanent-magnet machine with extended field-weakening capability," *IEEE Trans. Ind. Appl.*, vol. 39, no. 6, pp. 1704–1709, Nov./Dec. 2003.
[7] F. Leonardi, T. Matsuo, Y. Li, T. A. Lipo, and P. McCleer, "Design consideration and test result for a doubly salient PM motor with flux control," in *IEEE Ind. App. Soc. Annu. Meeting*, Oct. 2006.
[8] J. A. Tapia, D. González, R. Wallace, and A. Valenzuela, "Axial flux surface mounted PM machine with field weakening capability," in *Int. Conf. Electrical Machines, ICEM'2004*, Krakow, Poland.

Manuscript received January 9, 2008; revised April 25, 2008. Published August 20, 2008 (projected). Corresponding author: González-Lopez (e-mail: dgonzalez@DirectDriveSystems.net).

Delvis A. Gonzalez-Lopez (M'06) received the Electrical Engineer degree in 1997 and the Master in Science degree in 2001, both from Central University of Las Villas, Cuba. He received the Doctor in Engineering Science/Electrical Engineering degree in 2006 from the University of Concepcion, Chile.

Currently, he is an Electrical Engineer for Direct Drive Systems His research interests are electromagnetic analysis and design of electrical machines, primary permanent-magnet machines.

Juan A. Tapia (M'03) was born in Concepcion, Chile. He received the B.E.E. and M.E.E degrees in electrical engineering from the University of Concepcion, Concepcion, Chile, in 1991 and 1997, respectively, and the Ph.D. degree from the University of Wisconsin, Madison in 2002.

Since 1992, he has been with the Department of Electrical Engineering, University of Concepcion, as an Associate Professor. His primary areas of interest are electromechanical analysis and electrical machines design for ac adjustable speed applications.

Rogel Wallace (A'86) received the degree in electrical engineering from the Universidad Técnica Federico Santa Maria, Valparaiso, Chile, in 1966 and the Ph.D. degree in electrical engineering from Moscow Power Institute, Moscow, Russia, in 1976.

He was a Post-Doctoral Fellow in electrical machine design at the Moscow Power Institute. Since 1980, he has been with the Department of Electrical Engineering, University of Concepción, Concepción, Chile, where he is currently a Professor. His teaching and research interests include electrical machine design, power electronic, variable-frequency drives, and control systems theory applied to electrical drives.

Dr. Wallace received the Applied Science Award in 2001 from the Concepcion Municipality for his work.

Aníbal Valenzuela (M'93-SM'01) was born in Santiago, Chile. He received the degree in electrical engineering and the Master's degree in electrical engineering from the University of Chile, Santiago, Chile, in 1976 and 1978, respectively.

Since 1978, has been with the Department of Electrical Engineering, University of Concepción, Concepción, Chile, where he is currently an Associate Professor in the area of electric machines and drives. From August 1998 to June 1999, he spent his sabbatical leave at the University of Wisconsin, with the Wisconsin Electric Machines and Power Electronics Consortium (WEMPEC). He has several years of consulting activity in the pulp and paper, and mining industries. His current research interests include motion control of industrial drives, coordinated motion of multiaxis systems, sensorless control of ac drives, and thermal evaluation of induction motors.

Prof. Valenzuela was a recipient of the First Prize Paper Award for the best paper published in the IEEE TRANSACTIONS ON INDUSTRY APPLICATIONS in 2003, and of the First Place Paper Award at the 2006 IEEE Pulp and Paper Industry Technical Conference.